Inflatable Hip Protectors

By

Seyed Ehsan Arjmand Boroujeni
M. Sc., Isfahan University of Technology, 2009
B. Sc., Bahonar University, 2006

THESIS SUBMITTED IN PARTIAL FULFILLMENT OF
THE REQUIREMENTS FOR THE DEGREE OF

MASTER OF APPLIED SCIENCE

In the
School of Engineering Science
Faculty of Applied Sciences

SIMON FRASER UNIVERSITY

Summer 2012

Approval

Name: **Ehsan Arjmand**

Degree: **Master of Applied Science**

Title of Thesis: **Inflatable Hip Protectors**

Examining Committee:

Chair: **Dr. Behraad Bahreyni**

Assistant Professor of Engineering Science

_____

Dr. Siamak Arzanpour
Supervisor
Assistant Professor of Engineering Science

_____

Dr. Stephen Robinovitch
Supervisor
Professor of Engineering Science and Department of Biomedical Physiology and Kinesiology

_____

Dr. Krishna Vijayaraghavan
Internal Examiner
Professor and Associate

_____

Dr. Carolyn Sparrey
Internal Examiner
Professor and Associate

Date Defended/Approved: _____

Partial Copyright Licence

Abstract

Falls and fall-related injuries are crucial health problems among older adults, and hip protectors are designed to reduce fall-related injuries in this population. This thesis explores the technology of inflatable hip protectors with the aim to provide insight for future designers and manufacturers of these devices. The thesis comprises two studies. In the first, a mathematical model of an inflatable hip protector is developed. For system identification, a prototype of an inflatable hip protector is fabricated, and tested with an electromagnetic shaker. In the second study, a pelvis release experimental configuration is investigated to determine the effectiveness of inflatable hip protectors compared with commercially available hip protectors. Results suggest that airbags of moderate size – 20 cm x 10 cm – provide over three times the force attenuation of current passive devices. These results support ongoing efforts to develop inflatable hip protectors for older adults who are at high risk for falls and hip fracture.

Keywords: Hip fracture, Inflatable hip protectors; Modelling; Biomechanical effectiveness

Acknowledgements

I would like to thank my supervisors, Dr. Arzanpour and Dr. Robinovitch, for their excellent support during my graduate studies. Their professional attitude and positive personality continually inspired me, and their encouragements refreshed me in desperate moments. I would also like to thank Dr. Vijayaraghavan and Dr. Sparrey for kindly reviewing the thesis.

Table of Contents

List of Figures

List of Tables

Nomenclature

x	Vertical displacement of the airbag (m)
A_e	Effective area (m^2)
V	Volume of the airbag (m^3)
A_V	Volume change rate (m^2)
d	Diameter of vent (m)
F_r	Reaction force of the airbag (N)
P	Absolute pressure inside the bag (Pa)
P_g	Gauge pressure inside the bag (Pa)
P_0	Absolute initial pressure inside the bag (Pa)
P_{atm}	Atmospheric pressure (Pa)
V_0	Initial Volume of the airbag (m^3)
ρ	Density of gas inside the bag (kgm^{-3})
ρ_0	Initial density of gas inside the bag (kgm^{-3})
n	Polytropic index
R	Resistance coefficient
Q	mass flow (kg)
$\dot{Q}$	Mass flow rate (kgs^{-1})
C_P	Constant pressure specific heat ($Jkg^{-1}K^{-1}$)
C_V	Constant Volume Specific heat ($Jkg^{-1}K^{-1}$)

1: Introduction

Fall-related injuries such as bone fracture, subdural hematoma, soft tissue injury, and head injury pose serious health problems for older adults. These injuries reduce seniors' quality of life, often leading to chronic pain, dependence on others for daily activities, disability, and fatality [1]. Approximately one-third of those over 65 experience a fall at least once a year [2], and falls are recurring in half of those cases [3]. This statistic translates to nearly 1.4 million seniors in Canada who fell at least once in 2005, and the number of such seniors is projected to increase 2.35-fold by 2036 [4]. It is projected that by 2031, 24% of the Canadian population will be over 65, and it is estimated that nearly $4.4 billion dollars will be needed to cover the costs of their fall-induced injuries [5].

Among fall-related injuries, hip fracture has some of the most severe consequences. Nearly 20% of old people hospitalized for a hip fracture die within a year after the incident, and about 50% suffer from chronic consequences of hip fracture. The survivors are reported to become highly dependent on others for their basic daily activities [6, 7], resulting in significant decline in mobility, physical activity, and social interaction [8]. In other cases, even if a fall does not lead to significant injury, the affected senior may suffer from psychological trauma and renewed fear of falling, forcing him or her to be especially cautious in daily activities and to restrict routine daily activities [9]. Considerable growth in the senior population in Canada has resulted in an

exponential increase in the occurrence of hip fractures, creating an urgency in the battle to prevent hip fracture [10, 11].

1.1 Approaches to decreasing the risk of hip fracture

Considering the serious consequences of hip fracture, researchers of diverse backgrounds have investigated various approaches for countering the problem. For example, the emphasis by nutritionists, physicians and pharmacologists is to reduce the risk of hip fracture by focusing on enhancing the bone mineral density (BMD) and preventing bone loss. These investigations are important since statistical studies suggest that one in two women and one in five men over 50 will experience a fracture brought on by osteoporosis [12]. Nutritionists recommend a specific intake of calcium and protein as a potential solution [13], while research suggests that collective intake of vitamins such as vitamin D helps maintain bone heath [14]. Moreover, pharmacologists have proposed some medical intervention techniques such as parathyroid hormones, estrogen replacement therapy and oral strontium ranelate to increase bone density and, consequently, reduce the risk of hip fracture [15].

Biomechanics experts have also tried to prevent hip fracture through biomechanical interventions. Compliant floors in high-risk environments such as senior centers are an example of such interventions that have led to promising outcomes [16]. In addition, hip protectors represent a valuable biomechanical intervention to reduce facture risk of the proximal femur. These devices are typically made from plastic shields or foam pads placed over the greater trochanter (Figure 1- 2 and Figure 1- 2). Many studies report the use of hip protectors as a low-cost and effective way to prevent or reduce the

incidence of hip fractures in seniors in residential care services – like chronic care facilities, nursing homes, and homes for seniors [18]. Calculations show that use of hip protectors by 1,000 nursing home residents can prevent 27 hip fractures per year, amounting to a saving of approximately $270,000 [19]. Hip protectors are worn as a belt, or as a device under a skirt or pants [17]. The length, width, and thickness of passive hip protectors usually measure around 20 cm, 10 cm, and 5 cm. They are designed to cover the proximal femur, and are intended to absorb part of the energy of an impact to the hip or shunt the energy of the impact away from the greater trochanter to the soft tissues around the proximal femur.

A major drawback of hip protectors is, the elderly are reluctant to accept and use them. According to Patel et al., (2003), only a minority of older women in high-risk environments wear hip protectors [20]. The reasons people give for refusing to wear hip protectors are that the devices feel uncomfortable, they affect personal appearance, and more importantly, they may not actually prevent fracture during a fall.

Figure 1- 1: Passive hip protectors are made from plastic shields or foam pads placed over the greater trochanter. [http://www.activemobility.co.uk]

Figure 1- 2: 26 kinds of commercially available passive hip protector [23]

1.1.1 Inflatable hip protectors; challenges and rewards

Inflatable hip protectors are in principle similar to conventional automotive airbag systems. They consist of a folded bag that can be rapidly filled with air or other suitable gas [21], and an inflator that causes the bag to deploy. The design complexity of inflatable hip protections increases their overall cost compared with commercially available hip protectors. To be successfully marketed therefore, the performance of the inflatable devices must be substantially better than the commercially available units.

Although inflatable hip protectors are similar in principle to automotive airbags, certain design and deployment differences mark them apart. In automotive airbag systems, the accident detection is based on impact and acceleration sensors. The output of these sensors is processed with a microcontroller in real-time, and a signal is generated for the airbag deployment unit when a crash is detected. The airbag inflation begins by reacting sodium azide (NaN_3) with potassium nitrate (KNO_3), which releases hot nitrogen, which fills the airbag in only one-twenty-fifth of a second. Although this technology has been adopted successfully in the automotive industry, it cannot be used directly in wearable airbag applications. One reason is that the excessive heat generated as a result of chemical reaction during airbag deployment is not acceptable. In fact, the heat thus generated has caused injury to the body in some automotive applications, where all the reactions are confined and kept remote from the passengers. Using compressed gas such as CO_2 is another option, one that avoids the drawbacks of the automotive airbags. The first inflatable device to serve as a hip fracture protector is an airbag that was designed and marketed in Japan in 2008 [22]. The airbag is wearable, uses compressed air for inflation, and can be fully deployed in 0.1 seconds – meaning the time interval

between fall detection and airbag deployment. This airbag weighs 2.5 lb (1.1kg), and costs at least £700 (Figure 1- 4).

Figure 1- 3: The only available human airbag to prevent fall-related fractures, [http://www.dailymail.co.uk]

1.2 Risk factor

As discussed already, hip protectors are designed to absorb and shunt fall-induced energy to protect the femur. Two parameters determine the risk of hip fracture, or indicate the so-called risk factor: (1) the magnitude of the applied force, and (2) the femur strength [24]. The risk factor can be defined as (Figure 1- 4):

$$\text{Risk Factor} = \frac{\text{Impact force}}{\text{Required force to cause fracture}}$$

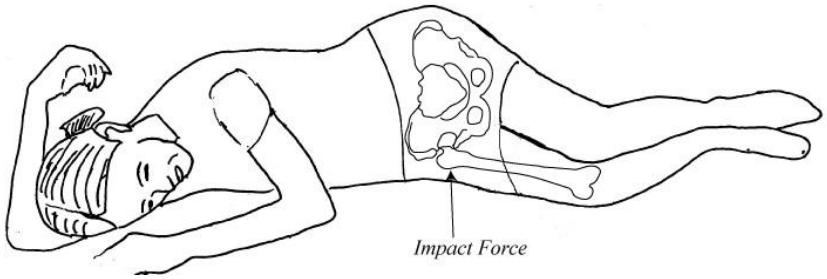

Figure 1- 4: The impact force applies on the femur, and the fracture occurs mostly at proximal femur

To determine the risk factor, therefore, we need to know the mechanical characteristics, or bone strength, of the femur, and the impact force.

1.3 Bone strength

Bone strength means the ability of a bone to tolerate loads. Generally, bone fracture occurs when the applied force is higher than the ultimate strength of the bone. Structural properties of bone such as mass, size, architecture, and surrounding tissue contribute greatly to bone strength, while trauma, aging and disease can also affect it [25].

The biomechanical properties of bones can be determined by mechanical experiments; bone samples are secured in an appropriate fixture and sample deflection is measured under loading conditions. The type of loading can be either tension, compression, bending, or torsion.

Many studies suggest a linear stress and strain relationship for bone structure in the beginning stage of loading; however, as the stress value increases, bone exhibits nonlinear characteristics. The transition between the linear and nonlinear behaviour occurs at the bone yield stress. In other words, yield stress divides the elastic region

(linear part) from the plastic region (nonlinear part). The point where the fracture ultimately occurs is called the failure point (Figure 1- 5) [26, 27, 28].

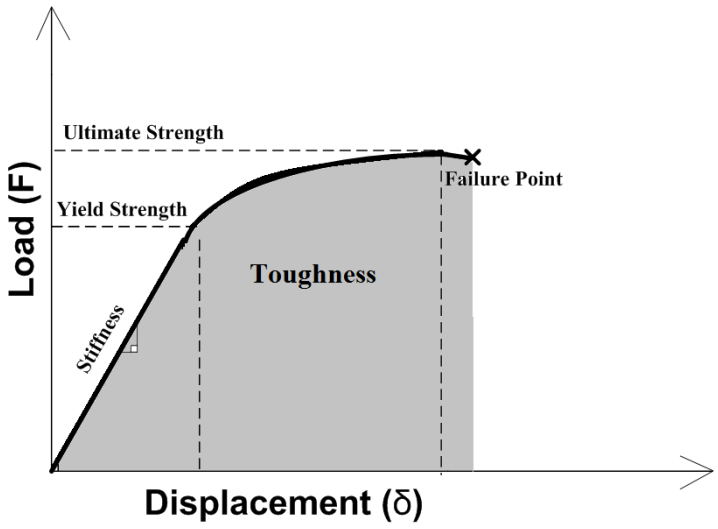

Figure 1- 5: Load-displacement behaviour; the stiffness is determined from the initial linear region; yield is the transition from linear to nonlinear behaviour; toughness is the shaded area.

In addition to producing mechanical stress-strain curves, other techniques are available to determine the risk factor. Toughness, defined as the energy absorbed by bone before its failure, can serve as another criterion for risk [29]. Moreover, for studying a rate-dependent material such as bone in a high-rate loading scenario similar to an actual fall, the impulse response is a more relevant approach for identifying ultimate strength [30].

1.3.1 The factors that contribute to ultimate bone strength

Bone strength depends strongly on age and sex of the patient, and on load direction and to a lesser extent load rating. Robinovitch et al. (2009) reviewed and summarized the results of 16 studies concerning cadaveric proximal femora strength. The

results are summarized in Table 1- 1; they reveal the importance of effective parameters in bone strength [31].

Lotz and Hayes (1990) conducted *in-vitro* experiments, independent of gender, with twelve pairs of fresh cadaveric proximal femurs; they reported ultimate strength ranging from 778 to 4040 N, mean 2110 N and Standard Deviation (SD) 1060 N [32]. Courtney et al. (1995) focused on the factors of age and loading rate. Concerning loading rate, their results suggest that for samples from both the elderly (mean age 73.5 and 7.4 (SD)) and young people (mean age 32.7 and 12.8 (SD) years), a higher loading rate (100 m/s versus 2 mm/s) increases the fracture strength by 20% . Moreover, age was found to be an important factor. For the elderly specimens, the fracture strengths were reported as 3440 and1330 (SD) (N) for a loading rate of 2 mm/s and, 4140 and1300 (SD) (N) for a loading rate of 100 mm/s; for the youth specimens and the same loading rates, the fracture strengths were 7200 and 1090 (SD), and 7800 and 1400 (SD), respectively [33]. Pinilla et al. (1996) investigated the importance of direction of applied force. Using a displacement rate of 100 mm/s, they showed that the load decreased by 24% due to an increase in loading angle from 0° to 30° on a femur neck; 4050 (SD 900) in, 3820 (SD 910) in 15^{o} and 3060 (SD 890) in 30^{o} to simulate forward, sideways and backward fallings respectively [34]. Pullkenin et al. (2006), studying the influence of gender on the peak force, examined 140 older cadavers of 77 females and 63 males. Their results suggest that the ultimate strength of the male specimen is 1.5 times greater than that of the female specimen [35].

1.4 Impact force

The magnitude of impact force is a key factor in a risk factor calculation and assessment of the biomechanical effectiveness of hip protectors. The magnitudes of the impact force reported in the literature are conjectural, because it is unethical to conduct *in-vivo* experiments. Such uncertainty among the reported magnitudes of impact force arises from both soft tissues around the hip and impact location, and direction [36]. For example, Nanakaku et al. (2005) reported the average of impact force on a 13-cm foam mattress for self-initiated side-way falls as 2252 N (442 SD), postero-lateral falls as 2498 N (457 SD), and posterior falls as 3247 N (587 SD) [37].

A proper mathematical model of a hip can be used as an alternative approach to predict the peak force magnitude. Such a model requires an adequate understanding of the biomechanics of falling to determine impact velocity, as well as authentic experimental data to identify model parameters such as effective mass, stiffness, and damping. For example, Robinovitch et al. (1997) identified parameters for different lumped parameter models – standard linear solid, Voigt, Maxwell, and spring – based on step response of a surrogate human pelvis/impact pendulum system of the force level between 50 and 350 N. They compared the prediction of the proposed models with the real situation through impact experiments in which the velocity of impact varied from 1.16 to 2.58 m/s and the corresponding measured impact forces were 1700 N and 5600 N, respectively. They realized that the mass-spring, Maxwell, and standard linear solid lumped parameters can predict the measured impact force with less than 3% error [38].

1.5 Thesis objectives

The goal of this study is, first, to drive a reliable mathematical model for inflatable hip protectors, and second, to develop and test the force attenuation, or biomechanical effectiveness, provided by inflatable hip protectors having different surface areas and inflation pressures.

Chapter 2 is allocated to mathematical modeling of an inflatable hip protector. To this end, the mathematical model of the system is derived based on the polytropic process equations, and the model is then validated through vibration experiments.

In Chapter 3 I describe the fabrication of inflatable hip protectors prototypes in three different sizes: small, medium, and large. Then I derive mechanical properties – stiffness and damping – of the prototypes with different experimental setups (inverted pendulum) and assess the proposed mathematical modeling described in Chapter 2.

In Chapter 4, I investigate the influence of geometry on force attenuation provided by inflatable hip protectors compared with that of commercially available padded hip protectors. For this purpose I used the Simon Fraser fall simulator setup in Injury Prevention and Mobility Laboratory.

1.6 Research novelty

Mathematical modeling and fabrication of inflatable hip protectors inspired from airspring systems is part of the novelty of this study. In this research I investigate the feasibility of using such complex hip protectors instead of passive padded units by examining their biomechanical effectiveness. In other words, results of this study are

expected to indicate the justification for supporting ongoing efforts to develop and implement inflatable hip protectors for older adults who are at high risk for falls and hip fracture.

Table 1-1: Several studies to measure bone strength in different conditions [31]

		Mean(SD) fracture force (N)			Mean(SD or range) age in years, sample size		
Study	Condition	Women	Men	Mixed	Women	Men	Mixed
Lotz and Hayes, 1990[e]				2,110(1,060)			69(9); $n=24$
Courtney et al. 1994[e]	Deformation rate=100 mm/s			4,100(1,600)			74(7); $n=8$
	Deformation rate=2 mm/s			3,440(13,30)			74(7); $n=8$
Bouxsein et al. 1995[e]				3,680(1,540)			76(59-96)[b]; $n=16$
Pinilla et al. 1996[e]	0° Load angle			4050(900)			79(11); $n=11$
	15° Load angle			3,820(910)			81(7); $n=11$
	30° Load angle			3,060(890)			74(11); $n=11$
Cheng et al. 1997,1998[d]		3140(1240)	4630(1550)	3,980(1,600)	71(15); $n=28$	67(15); $n=36$	69(15); $n=64$
Bouxsein et al. 1999[e]		1997(1127)	3593(1614)	2,636(1,534)	82(13); $n=16$	78(10); $n=10$	81(12); $n=26$
Keyak et al. 2000[e]				2,400[a]			70(52-92)[a]; $n=17$
Lochmuller et al. 2002[d]		3,070(1060)	4,230(1530)		82(9); $n=63$	76(11); $n=42$	
Eckstein et al. 2004[d]				3,925(1,650)			79(11); $n=54$
Heini et al. 2004[e]				2,499(6,95)			76(7); $n=20$
Manske et al. 2006[e]				4,354(1,886)			69(16); $n=23$
Pulkkinen et al. 2006[d]		2,821[a]	4,209[a]	3,472[a]	82; $n=77$	79; $n=63$	81; $n=140$
Bouxsein et al. 2007[e]				3,353(1,809)			81(11); $n=49$
Pulkkinen et al. 2008[d]	Cervical fx	2,879(1,117)	4,079(1,165)		82(11); $n=34$	78(11); $n=28$	
	Trochanteric fx	3,053(976)	5,506(1374)				
Across study average		2,827	4,375	3,392	80	76	76

[a] SD not provided
[b] Range (not SD) reported
[c] Specimens were stored fresh-frozen
[d] Specimens were embalmed in alcohol/formalin
[e] Specimens were stored frozen, but the authors did not specify fresh versus embalmed.

2: Mechanical Modelling of Inflatable Hip Protectors

Systems modeling and analysis are tools used in most engineering disciplines [39]. It provides insight into system characteristics and helps engineers investigate and better understand the parameters for predicting an output without conducting tests.

An inflatable hip protector is a multivariable and complex system. For systems like this, detailed models do not generally provide a clear understanding of the effects of various parameters on system behavior. A common approach in modeling these systems is to neglect the least important parameters by making valid assumptions and simplifying the overall system into a realistic model by describing it in terms of the parameters that most affect the system. On the other hand, making unrealistic assumptions and disregarding many parameters in the system affect the accuracy of the model and make it incapable of capturing the essential behavior of the system. A fair balance between the complexity and accuracy of the model must therefore be determined.

In this Chapter I obtain a mathematical model of inflatable hip protectors based on valid assumptions used for modeling similar systems. To accomplish this goal, I take advantage of previous studies on airsprings that are highly similar to airbag systems. Then the model is validated through experiments.

In terms of mathematical modeling, there are many similarities between airspring systems used in trucks and heavy vehicles and inflatable hip protectors. As indicated in

Figure 2- 1, both systems consist of a flexible membrane for capturing pressurized air to attenuate applied dynamic forces.

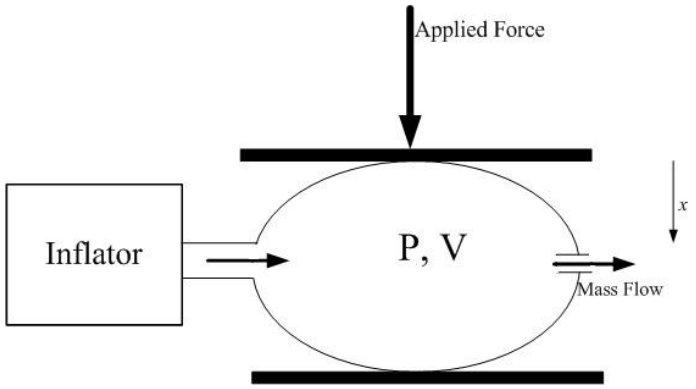

(A)

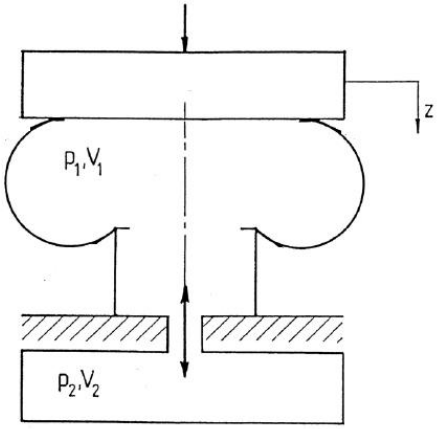

(B)

Figure 2- 1: General configuration of inflatable hip protectors and an airspring [41, 42].

Inflatable hip protectors consist of three main elements: an inflator, a bag, and a vent (Figure 2- 1). The impact force in the vertical direction (shown as *x*) causes the bag to deflate. In this airbag, the inflator produces gas when a fall is detected.

Simultaneously, the vent allows the air outflow to damp the high internal energy, to prevent of hip fracture [40]. The airspring system consists of a bag, a reservoir, and an orifice with the same functions as bag, inflator, and vent, respectively.

2.1 Mathematical modeling of airspring systems

Both systems also undergo the same thermodynamic process, or polytropic process, which is

$$PV^n = \text{Constant} \tag{2- 1}$$

where *P* and *V* are the pressure and volume of the air inside the bag [42]. In equation (2-1) the polytropic index (*n*) can take any real number, depending on the process. For certain values of the polytropic index, the equation represents common thermodynamic processes. For example, *n* equaling 0, 1, and infinity results in isobaric (constant pressure), isothermal (constant temperature), and isochoric processes, respectively. In the case where the system does not exchange heat with the surrounding, $n = \gamma$, where γ represents the adiabatic index and can be defined as

$$\gamma = \frac{C_p}{C_v} \tag{2- 2}$$

where C_p and C_v are specific heats of the gas inside the inflated airbag at constant pressure and volume, respectively [43].

In dynamic processes, the rate of the process determines the type of polytropic system. For example, if the process is very slow, the system is able to exchange heat with the environment and the temperature remains constant (isothermal). On the other hand, if

the process is very fast, the system does not have sufficient time to exchange energy with the environment and, therefore, the process is closer to adiabatic. In that case, *n* is a function of the frequency of the gas expansion and compression, which generally varies between 1 (isothermal) and γ (adiabatic). For simplicity, in our studies a fixed number is used for *n* based on the fact that the system undergoes an adiabatic process. In addition, it is assumed that high-frequency dynamic processes for the airbag system occur at more than 0.2 Hz. As a result, the processes for those frequencies can be considered adiabatic because the system develops so quickly that the heat generated due to air compression and expansion has little time to exchange between the system and the environment – an adiabatic process in which $n=\gamma$ [44]. In fact, the impact force from falls occurs in less than 1 sec, and can be considered a high-frequency process [45].

The airspring and inflatable hip protector systems shown in Figure 2- 1 can also be presented by the simplified configuration shown in Figure 2- 2. In the new configuration, the effective area of the airbag during impact is modeled by the area at the top of the bag. Moreover, the vent is modeled as a valve so that the mass flow can be studied and measured as a separate parameter. The new model makes it easier to comprehend the mathematical modeling of the airbag.

The equation governing the system based on the adiabatic process for an ideal gas is ([42])

$$P_0(V_0 - \frac{Q}{\rho_0})^n = P(V_0 - A_V x)^n \qquad (2\text{- }3)$$

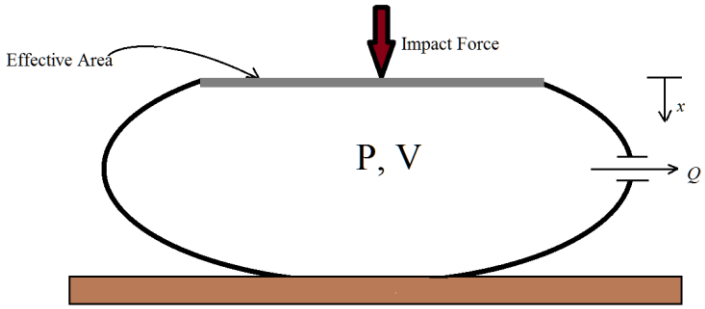

Figure 2- 2: Simplified configuration of an airspring or vented inflatable hip protectors

where $V_{0,}$ P_0 and ρ_0 represent the initial volume, pressure, and density, respectively, and A_V represents the variation of volume with respect to displacement; that is,

$$A_V = \frac{dV}{dx} \tag{2- 4}$$

and mass Q represents the flow of air from the membrane, which is

$$Q = Q_{in} - Q_{out} \tag{2- 5}$$

where Q_{in} and Q_{out} represent inflowing and outflowing mass flow, respectively. Equation (2- 3) can be written in the form

$$P = P_0 \left[\frac{\rho_0 V_0 - Q}{\rho_0 (V_0 - A_V x)}\right]^n \tag{2- 6}$$

For a small displacement, meaning$V_0 \gg A_e x$, (2-5) can be simplified using Taylor series expansion:

$$P = P_0 \left[1 + n\frac{\rho_0 A_V x - Q}{\rho_0 V_0}\right] \quad (2\text{- }7)$$

At the same time, the dynamic reaction force (F_r) of the airbag, from where the impact is induced, can be determined as

$$F_r = P_{Gage} A_{Effective} - F_{r_{Static}} \quad (2\text{- }8)$$

where $F_{r_{Static}}$ is a static part of the reaction force and is equal to

$$F_{r_{Static}} = (P_0 - P_{atm}) A_{e_{Static}} \quad (2\text{- }9)$$

Therefore,

$$F_r = (P - P_{atm})(A_e + A_x x) - (P_0 - P_{atm}) A_e \quad (2\text{- }10)$$

where A_x is the variation of effective area with respect to displacement ($A_x = \frac{dA_e}{dx}$) Consequently, after substituting equation (2- 7) into (2- 10) , we have

$$F_r = \left(\frac{nA_e A_V P_0}{V_0}\right)\left(x - \frac{Q}{\rho_0 A_e}\right) + (P_0 - P_{atm})(A_x x) \quad (2\text{- }11)$$

To simplify the mathematical model, new parameters are defined as

$$y = \frac{Q}{\rho_0 A_V} \quad (2\text{- }12)$$

$$K_1 = \frac{nA_e A_V P_0}{V_0} \quad (2\text{- }13)$$

$$K_2 = (P_0 - P_{atm}) A_x \quad (2\text{- }14)$$

Thus, equation (2- 11) can be rewritten as

$$F_r = K_1(x - y) + K_2 x \tag{2- 15}$$

In addition, the equation for the mass flow rate through the vent is

$$\dot{Q} = \frac{P - P_{atm}}{R} \tag{2- 16}$$

where *R* is the vent resistance. Substituting equation (2- 7) into (2- 16) results in

$$R\dot{Q} = (P_0 - P_{atm}) + \frac{nA_V P_0}{V_0}\left[x - \left(\frac{1}{\rho_0 A_V}\right)Q\right] \tag{2- 17}$$

Using the parameters defined in equations (2- 12) to (2- 14), equation (2-16) becomes

$$B\dot{y} = K_1(x - y) + F_e \tag{2- 18}$$

where

$$F_e = (P_0 - P_{atm})A_e \tag{2- 19}$$

$$B = R\rho_0 A_e A_V \tag{2- 20}$$

and where $\dot{y}$, as shown in equation (2- 12), is related to the effective area and the rate flow. This means that the flow rate $\dot{Q}$ depends on the area of the vent and the inside pressure.

According to equations (2- 15) and (2- 18), the lumped-parameter model of the system consists of two springs. The first spring reflects the geometric changes, and the

second represents the effect of initial pressure inside the airbag. Figure 2-4: shows the lumped parameter model of the system. In this model, the damping is the result of the loss of the air momentum inside the bag due to the mass outflow. Other energy losses, such as heat generation, are neglected in this model [42, 46, 47].

2.2 Mathematical modeling of inflated inflatable hip protectors

In a simplified case the inflatable hip protector does not have a vent, so to obtain its mathematical equation we need only eliminate the effect of vent in the vented model. Therefore, equation (2- 3) becomes

$$PV^n = P_0 {V_0}^n \tag{2- 21}$$

Subsequently, the reaction force of the system is

$$F_r = \left(\frac{nA_e A_V P_0}{V_0} + (P_0 - P_{atm})(A_x) \right) x \tag{2- 22}$$

It can also be concluded that

$$K = \frac{nA_e A_V P_0}{V_0} + (P_0 - P_{atm})(A_x) \tag{2- 23}$$

Equations (2- 22) and (2- 23) suggest that the stiffness is highly related to geometrical parameters – volume and effective area – and to initial pressure inside the bag for both vented and unvented inflatable hip protectors. The only significant difference is the loss of energy in the vented system. This model will be validated experimentally.

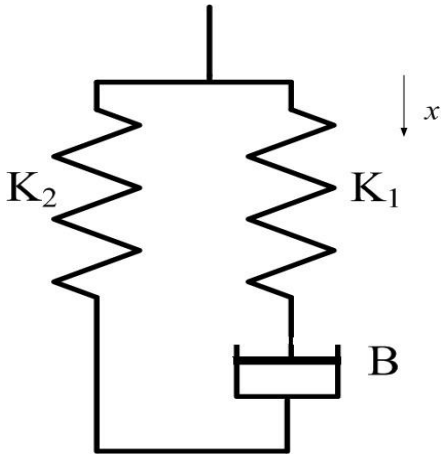

Figure 2-4: Lumped parameter model of vented airbag and airspring systems [47]

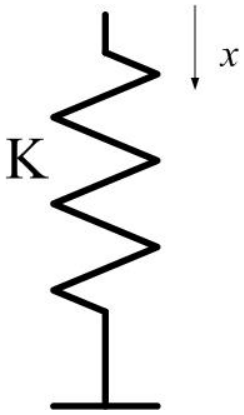

Figure 2- 4: Lumped parameter model of inflated airbag system without vent

2.2.1 Geometric parameters; effective area and volume change rate

According to the models, the effective area or load-carrying area is an important geometric parameter which plays an important role in the performance of the airbag, and it should be precisely determined for dynamic analysis. The role of the effective area can be simulated by a piston with the same cross sectional area (Figure 2- 2). The effective area of an airbag system can be obtained experimentally by dividing the applied force on the airbag by its pressure (gauge) [46]

$$A_e = \frac{F_x}{P_g} \tag{2- 24}$$

A_V can also be calculated from equations (2- 13) and (2- 24) by substituting effective area and stiffness [46].

$$A_V = \frac{dV}{dx} \tag{2- 25}$$

2.3 Experimental analysis

Experimental analyses are essential for parameter identification that is effective area, and validating the theoretical models and simulations. In our experiments, an electromagnetic shaker (LDS- V406) is used to produce accurate and repeatable displacement excitations at a given frequency. This actuator is controlled by LASERUSB with 24-bit precision, as shown in Figure 2- 5. The controller enables various dynamic tests such as sweep sinusoidal excitation for frequencies over 5 Hz. The experimental tests are conducted in the frequency range 5 to 25 Hz valid for inflatable hip protectors modeling, whereas the natural frequency of the hip which is around 6 Hz and falls into this range of frequency [48]. A load cell (Kistlet Model 9712A5000) is used to measure the transmitted force. Also, a LVDT (Linear Variable Differential Transformer) is used to measure the shaker displacement. The experimental arrangement is also instrumented with two pressure sensors. One of the pressure sensors has a low range (0-5 PSI) to achieve the high accuracy required to record the initial pressure (Model ASDX005, SenSym ICT), while the other sensor has a higher range (0-100 PSI) to measure dynamic pressure (Model DPX 101, OMEGA Company). A custom made manifold is fabricated to connect the airbag system to compressed air, and a valve is placed to connect and disconnect the compressor.

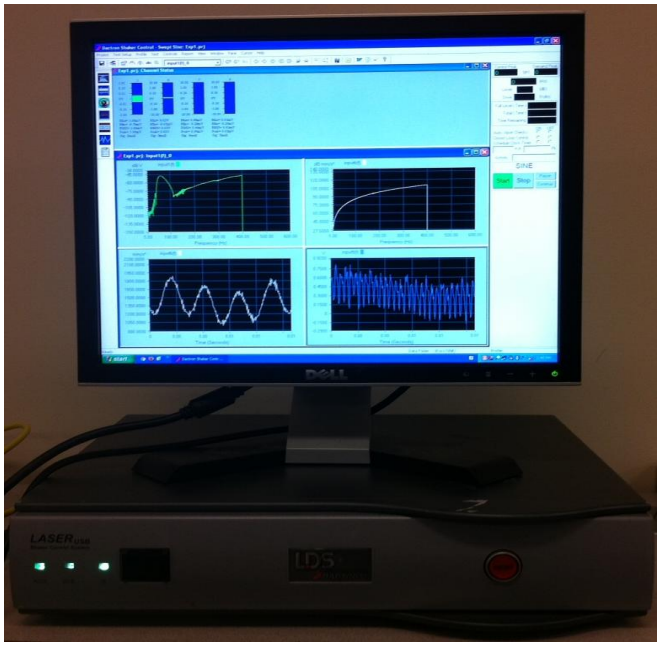

Figure 2- 5: LaserUSB system which has a USB 2.0 interface for easy PC connectivity

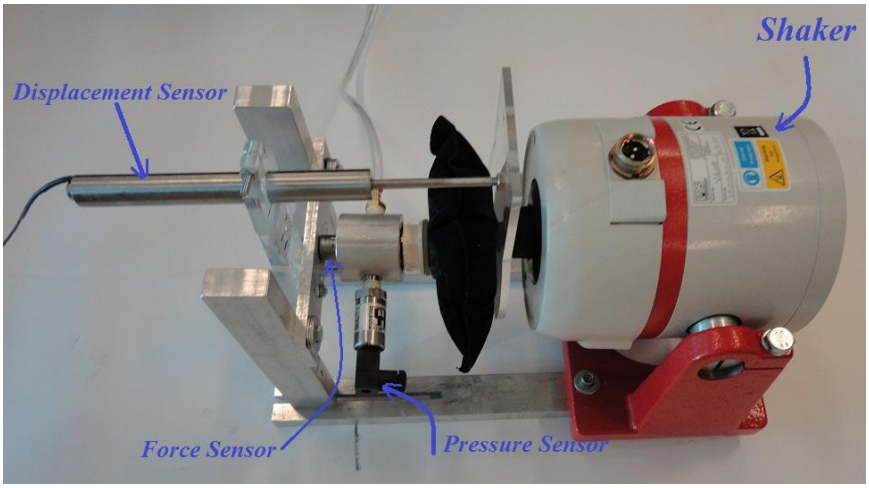

Figure 2- 6: The setup utilized to study an inflatable hip protector

Only unvented inflated inflatable hip protectors were tested. Theoretically, the system is expected to behave like a spring, with the damping negligible due to high frequency of excitation, which exceeds 5 Hz, meaning the heat exchange of the bag (due

do contraction and expansion of the air inside the bag) and the surrounding environment is negligible.

2.3.1 Experimental results

The main objective of the experimental modeling is parameter identification**.** As already noted, the effective airbag area parameter should be determined experimentally. In this experiment, we investigated the roles of several parameters such as displacement, frequency and initial pressure on the effective area. According to the experimental results, the effective area depends merely on displacement amplitude, with the contributions of frequency and initial pressure negligible (Figure 2- 7 and Figure 2- 8).

We used Bode plots to observe the behaviour of the system, which is an effective approach to study frequency response. These plots are in log-log format, and the shape of gains and phase plots represents system behaviour [49]. For example, constant gain with zero phase represents the behaviour of a pure spring. If a source of energy loss exists, then the Bode plot is a straight line at low frequencies, which gradually becomes a line of 20 dB slope. The phase shift of the system between the low and high frequencies is 90 degree. Figure 2- 9 to Figure 2- 13 represent the Bode plots of the system under different displacement amplitude excitations; as indicated, the corresponding bode plots suggest that the system behaves like a spring, and the damping of the system is almost negligible.

The experimental results confirm that the airbag behaves like a spring. The approximately zero phase changes in those graphs also suggest that the damping coefficient is negligible. According to Figure 2- 14, the stiffness of the spring can be considered linear, and is function of initial pressure inside the bag.

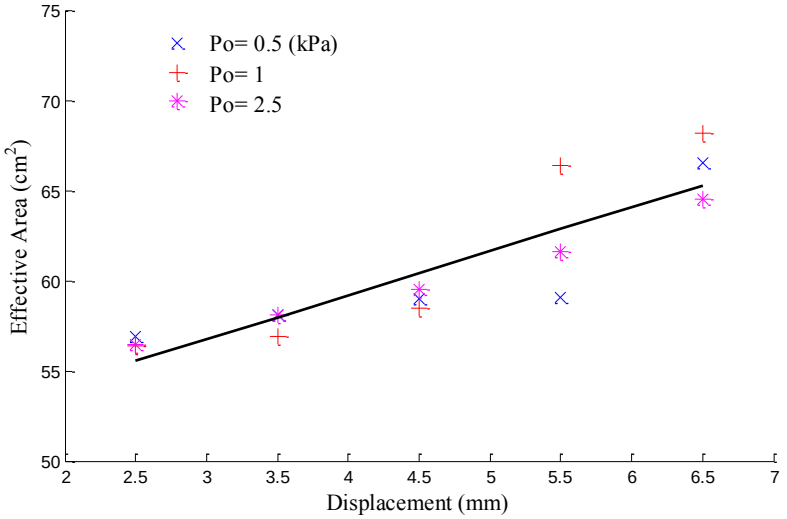

Figure 2- 7: Data suggest that the effective area depends on displacement (A_e) measured by ration of gauge pressure and reaction force ($\boldsymbol{A_e = \frac{F}{P_g}}$).

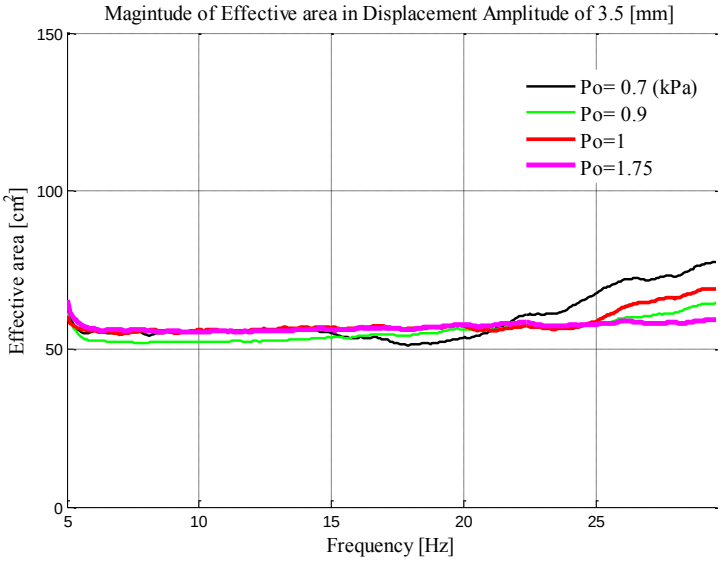

Figure 2- 8: Effective area is independent of pressure and frequency

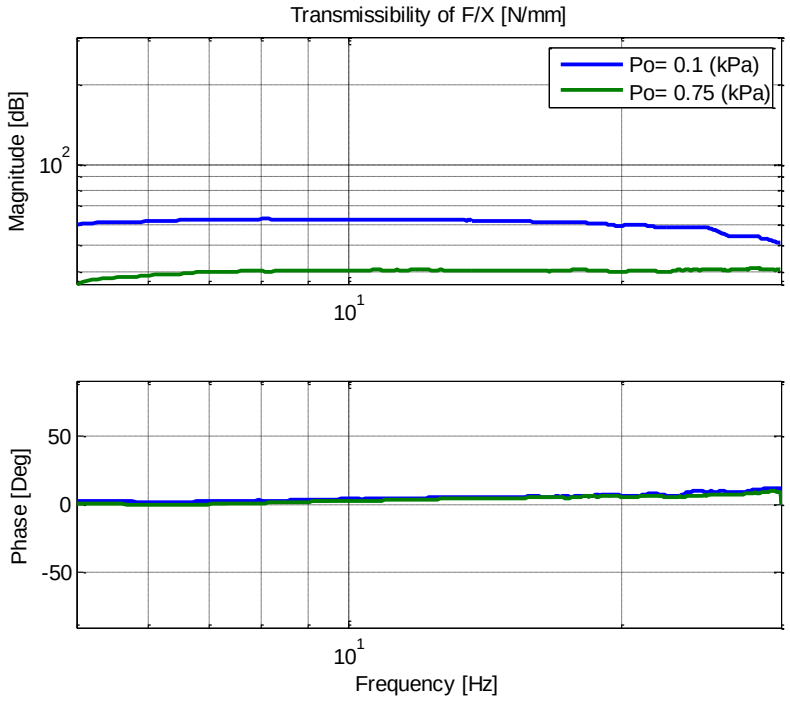

Figure 2- 9: Bode plot while the amplitude of displacement is 2.5 (mm)

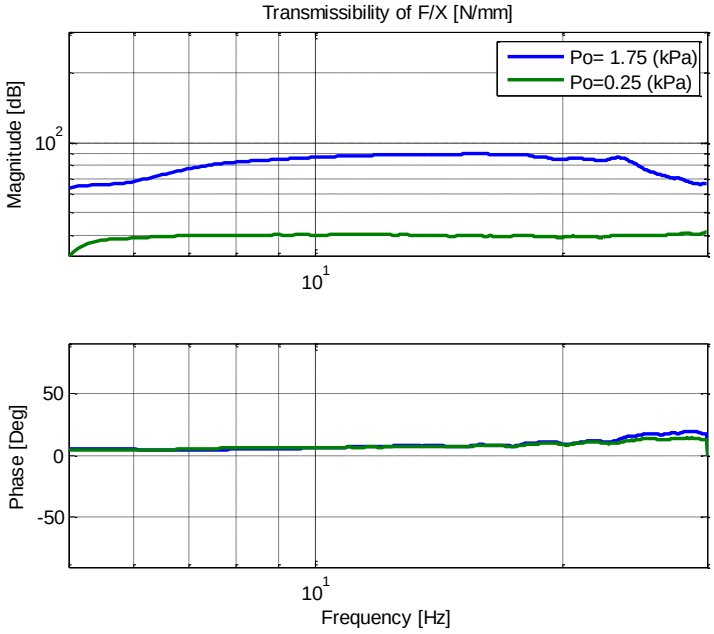

Figure 2- 10: Bode plot while the amplitude of displacement is 3.5 (mm)

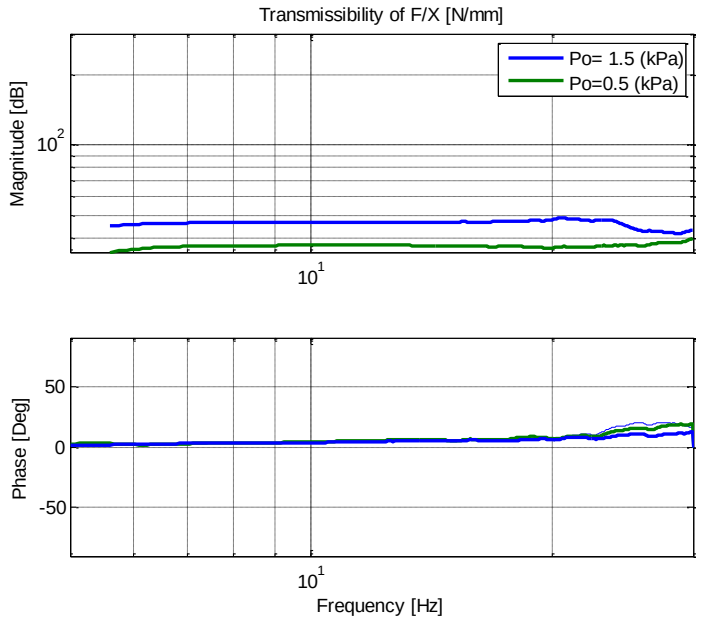

Figure 2- 11: Bode plot while the amplitude of displacement is 4.5 (mm)

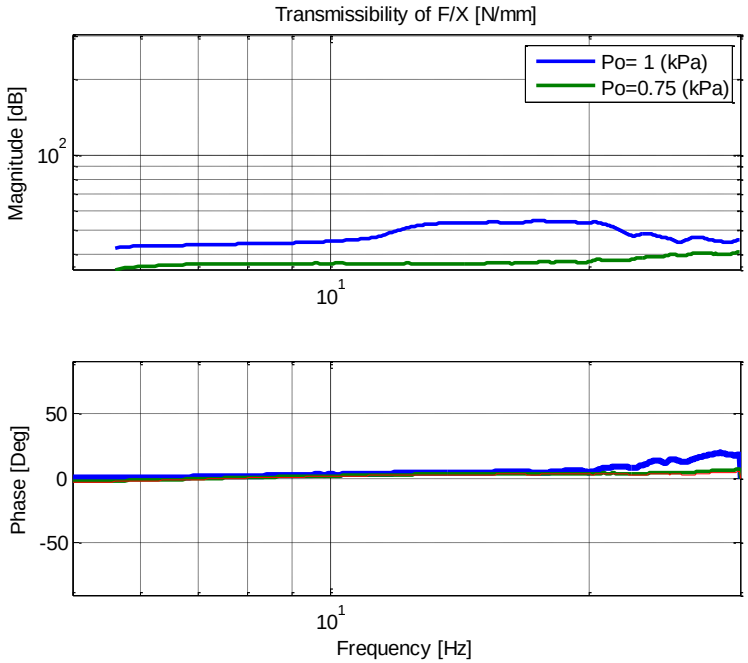

Figure 2- 12: Bode plot while the amplitude of displacement is 5.5 (mm)

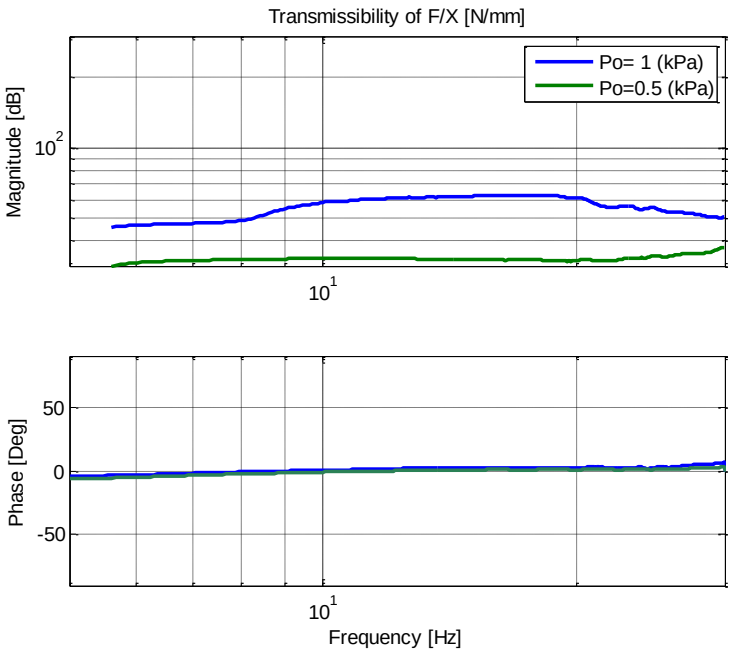

Figure 2- 13: Bode plot while the amplitude of displacement is 6.5 (mm)

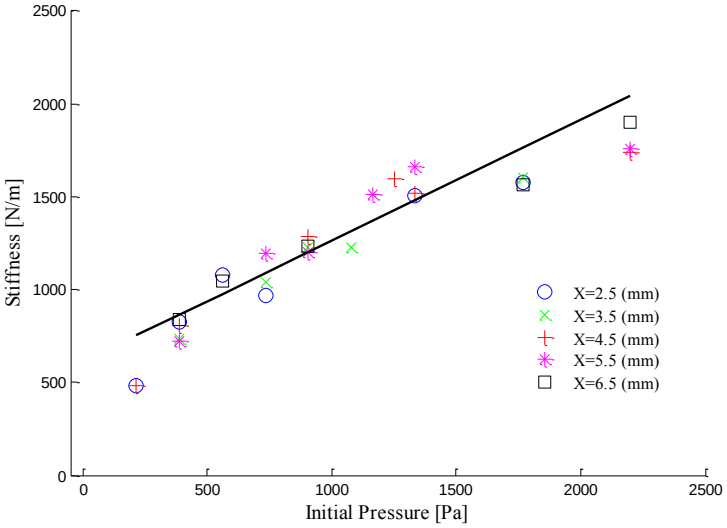

Figure 2- 14: Relation of stiffness with displacement and initial pressure

To determine A_V, we used experimental results and equation (2- 23). The results are summarized in Table 2- 1. The data suggest that A_v is almost 10 times smaller than A_e, indicating the probability of membrane bulging during dynamic loading – as was seen during experiments.

Table 2- 1: The calculated magnitudes of A_V, through experimental data and equation (2- 23) in amplitude of 4.5 (mm)

Initial Pressure (kPa)	**Stiffness (N/m)**	A_e **(cm^2)**	A_V **(cm^2)**
0.5	800	58	5
1	1200	58	5.5
1.5	1500	58	6.5

2.4 Conclusion

The experimental results lead to the conclusion that the spring model shown in Figure 2- 4: is a realistic model that describes the mechanical behaviour of the inflatable hip protector, while the damping of the system is negligible. The magnitude of stiffness can be determined by vibration test analysis.

The stiffness of the unvented inflatable hip protectors is a function of initial pressure and of the airbag geometry. In addition, the system under operating conditions behaves almost linearly (Figure 2- 14).

3: Biomechanical Effectiveness of Inflatable Hip Protectors of Different Sizes

Wearable hip protectors, being padded garments, are a promising approach to hip fracture prevention. These devices reduce risk of fracture by attenuating the impact force applied to the proximal femur during a fall. They are made from either soft or hard foam rubber or plastic materials. Soft-shell hip protectors reduce the force applied to the proximal femur by decreasing the local stiffness over the greater trochanter and absorbing impact energy. In contrast, hard-shell hip protectors shunt energy away from proximal femur and into the surrounding soft tissues, where it can be safely absorbed ([52] , [53]). The biomechanical effectiveness of, or force reduction provided by, such products depends on their geometry – for example, surface area and thickness – and material properties [51], as well as on external factors such as impact velocity, soft tissue properties, and pelvic surface geometry ([17], [53], [54]). Using the hip impact simulator at Simon Fraser University, Laing et al. in 2011 [51] conducted a comprehensive comparison of the biomechanical effectiveness of 26 commercially available hip protectors. They simulated three different fall severities by adjusting the impact velocity to 2, 3, and 4 m/s, and found that at an impact velocity of 3 m/s, the biomechanical effectiveness ranged from 2.5% to 40%. At 2 ms, the best available hip protector provided 48.3% force attenuation, with an average force attenuation of 20.2%.

It is likely that inflatable hip protectors would provide considerably greater force attenuation than current passive devices. Due to their more complex design and

fabrication challenges, and likely their cost to consumers, they must provide considerably more protection than do currently available devices, to justify the feasibility of this option. In this chapter, I examine the biomechanical effectiveness of inflatable hip protectors using the Simon Fraser University fall impact simulator. I also examine how biomechanical effectiveness is influenced by inflatable hip protector geometry, initial pressure, and impact velocity. These laboratory studies provide needed evidence of the biomechanical advantage of inflatable hip protectors over commercially available passive devices.

I first describe the Simon Fraser University fall impact simulator, and then describe the prototype manufacture and testing of three inflatable hip protectors of different sizes. Next I describe measures to characterize mechanical properties – stiffness and damping – and force attenuation provided by each device, and discuss the results.

3.1 Fall impact simulator configuration

The Simon Fraser University fall impact simulator consists of a pendulum and surrogate pelvis released by an electromagnet from different initial angles of inclination, simulating different fall heights, to hit the ground horizontally, as shown in Figure 3- 1. The surrogate pelvis comprises foam-rubber soft tissues and an instrumented proximal femur (Sawbones, Vashon, WA, USA). Surface geometry and local variation in soft tissue stiffness match average measurements from older women to within one standard deviation. The surrogate pelvis is connected to the pendulum via leaf springs that simulate the compliance of the pelvis.

Impact velocity is varied by adjusting the angle of the pendulum before release, and is measured by a rotary variable inductance transducer (Shaevitz RVIT 15-1201). The force applied to the femoral neck is measured by a load cell (Kistler Model 9712A5000, Amherst, NY, USA), and the total impact force is measured with a force plate (model 2535-08, Bertec Corp., Columbus, OH, USA).

The surrogate pelvis itself consists of a simulated proximal femur and bonded layers of foam rubber, simulating the soft tissues – skin, fat, and muscle – surrounding the bones of the femur and pelvis. The material, thickness, and shape of the layers were chosen to match the stiffness and geometry of an old person's hips, as reported by Laing et al. ([53].). Moreover, the stiffness of pelvis, trunk and lower extremities is simulated through a leaf spring located between the surrogate pelvis and the pendulum, producing a total effective stiffness of 42.2 kN/m ([55], [56]). The effective mass of the pendulum is 28 kg, close to the average reported effective mass of young adults measured during side-way falls [55].

The inflatable hip protector is mounted on the force plate as depicted in Figure 3-2 and Figure 3- 3. It is connected via tubes to a pressure sensor (range 0-5 PSI, Model ASDX005, SenSym ICT) that records the initial inflation pressure, and to an air compressor. The inflatable hip protectors being studied were made of a type of non-elastic vinyl. They were manufactured in small, medium, and large sizes, having respective surface dimensions of 105 mm x 110 mm, 145 mm x 140 mm, and 270 mm x 140 mm, as shown in Figure 3- 4. Fabrication of the prototypes is explained in the next chapter.

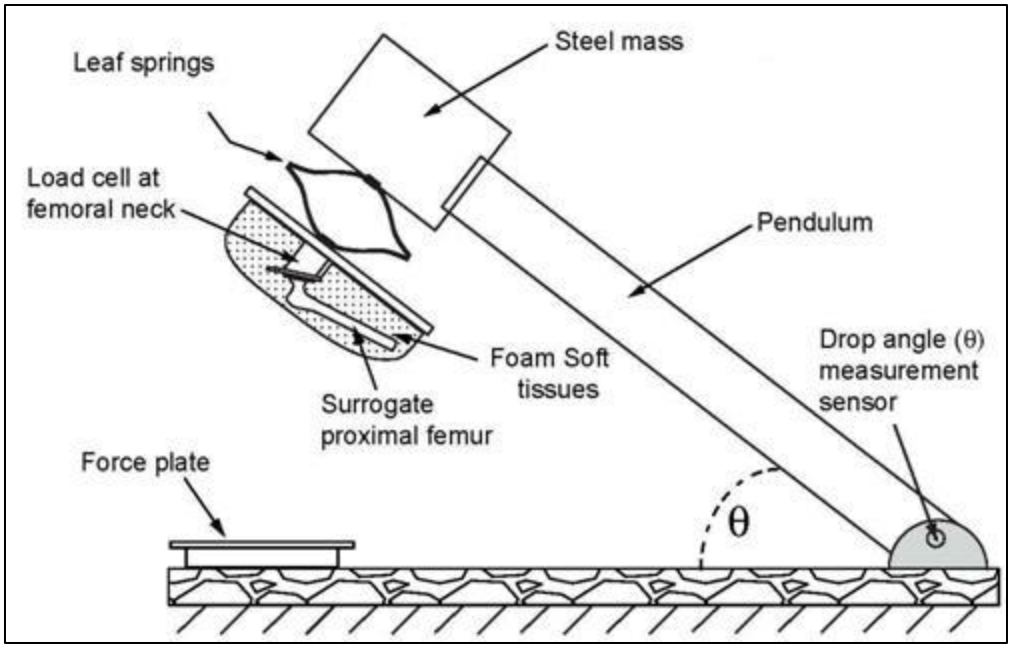

Figure 3- 1: Simon Fraser University hip impact simulator. A surrogate pelvis is mounted on the end of an impact pendulum. A load cell located in the femoral neck measures the force applied to the proximal femur during a simulated sideways fall.

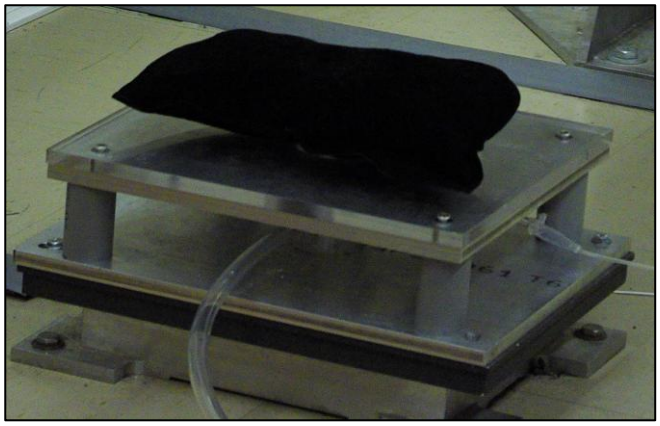

Figure 3- 2: Inflatable hip protector mounted on a force plate and connected to a pressure sensor and air compressor.

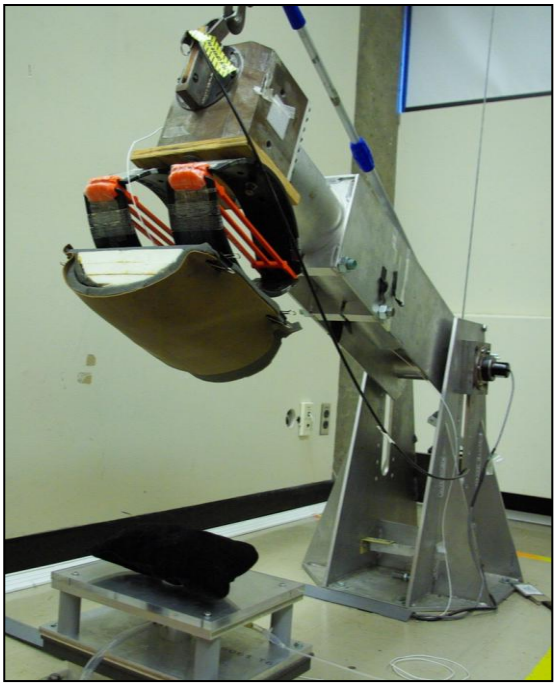

Figure 3- 3: Inflatable hip protector and impact pendulum setup in measurements of the biomechanical effectiveness of the hip protector.

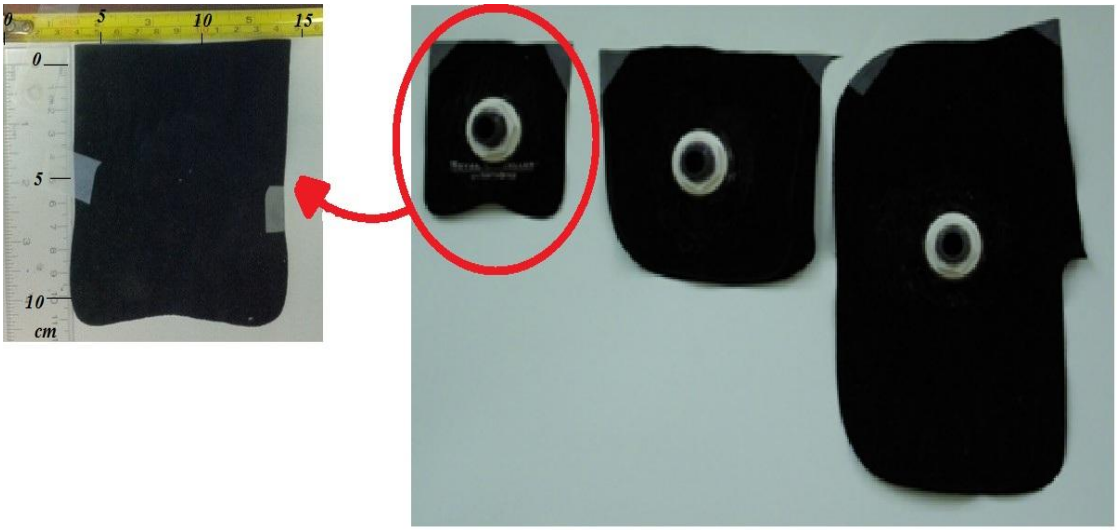

Figure 3- 4: The inflatable hip protectors examined in this study have surface dimensions of 105 mm x 110 mm, 145 mm x 140 mm, and 270 mm x 140 mm.

3.2 Biomechanical effectiveness of inflatable hip protectors

In additional experiments, I used the SFU Hip Impact Simulator to measure the force attenuation provided by each inflatable hip protector, and a selection of common passive hip protectors, under conditions that simulate a sideways fall. In these tests, a surrogate pelvis, matching the surface profile and soft tissue properties of older women, was attached to the impact pendulum, following the approach used by Laing et al. (2011) [49]. I also examined the effect of initial inflation pressure on force attenuation provided by each inflatable hip protector. In each condition, I calculated the biomechanical effectiveness of each hip protector as

$$\boldsymbol{Biomechanical\ Effectiveness} = \frac{\boldsymbol{Peak\ femoral\ force\ in\ unpadded\ condition - Peak\ femoral\ force\ in\ padded\ condition}}{\boldsymbol{Peak\ femoral\ force\ in\ unpadded\ condition}}$$

3.2.1 Method

An initial series of measurements was conducted in the unpadded condition to determine whether the peak impact forces were similar to that reported by Laing et al. (2011) [51]. Table 3- 1 indicates that the data recorded with the current setup matched well those obtained by Laing et al.

Table 3- 1: Calibration of the Hip Impact Simulator, showing peak forces in trials involving impact velocities of 1, 2, and 3 m/s that are consistent with those reported by Laing et al., 2011.

Impact Velocity (m/sec)	Force Plate (N)	Load Cell (N)
1	1220 1340	800 745
2	2150 2170	1500 1380
3	2850 2925	2050 1960

Trials were then conducted with each of three inflatable hip protectors secured and centred over the greater trochanter of the surrogate pelvis. The hip protectors were completely sealed and the initial pressure was recorded before the pendulum hit the force plate. The initial release angle of the pendulum was adjusted to provide an impact velocity of either 1, 2, or 3 m/s. Measurements were recorded with the large hip protector at impact velocities of 1, 2, and 3 m/s. For the small and medium protectors, measurements were acquired for impact velocities of 1 and 2 m/s only, based on the concern that an impact velocity of 3 m/s might rupture of the hip protector and damage the test system.

3.2.2 Results and discussion

Force attenuation for the small inflatable hip protector was observed to be equal to the force attenuation provided, on average, by commercially available passive hip protectors at an impact velocity of 2 ms (Figure 3- 5). The medium and large inflatable protectors provided 1.5 times and 3 times the force attenuation provided on average by passive devices. At an impact velocity of 3 m/s, the large inflatable hip protector again provided about 3 times the force attenuation of commercially available devices (Figure 3-6).

As shown in Figure 3- 7, in addition to geometry, impact velocity influences force attenuation, because the results indicate that force attenuation in the inflatable designs increases with increasing impact velocity – contrary to what is observed with passive devices. For example, the percentage of force attenuations for large, medium, and small

inflatable hip protectors at an impact velocity of 1 m/s are 58%, 29% and 18%, respectively, whereas at an impact velocity of 2 m/s, the values increase to 61%, 32.5%, and 22.5% , indicating a direct relation between impact velocity and force attenuation.

As shown in Figure 3- 8, the initial pressure had minimal effect on force attenuation. This finding suggests that, so long as there is enough air inside the bag to allow for separation of the inflatable hip protector membrane in all directions, the protector should provide effective force attenuation.

Table 3- 2: Measured peak forces in different Inflatable hip protector types

Impact Velocity (m/s)	Measured peak forces in different Inflatable hip protector types (N)					
	Small		**Medium**		**Large**	
	Femur	Force Plate	Femur	Force Plate	Femur	Force Plate
1	661.66 (SD 7.39)	1155.3 (SD 11.89)	572.67 (SD 8.28)	1089.5 (SD 14.5)	335.6 (SD 8.17)	1017.8 (SD 32.43)
2	1196.8 (SD 8.01)	1987.8 (SD 7.36)	1043 (SD 8.16)	1969.5 (SD 3.83)	605.33 (SD 7.23)	1958 (SD 25.86)
3					880.4 (SD 7.16)	2660.4 (SD 7.20)

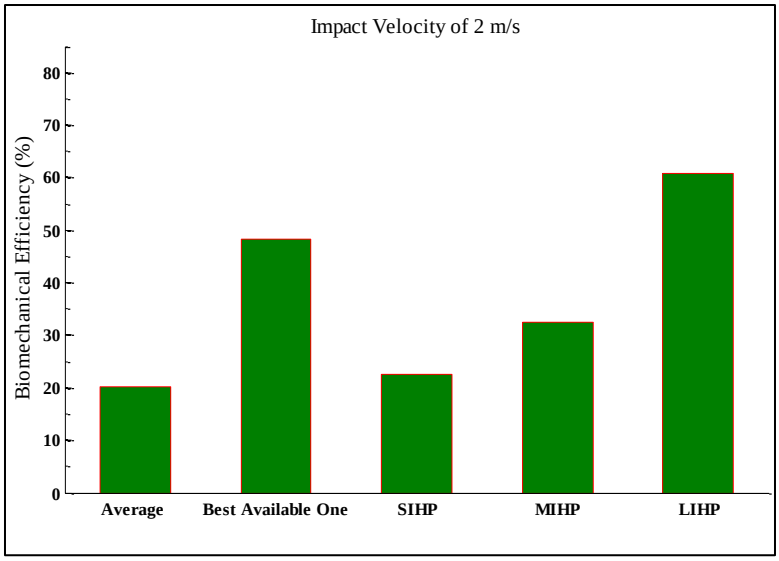

Figure 3- 5: Comparison of the biomechanical effectiveness (attenuation in peak femoral force) at an impact velocity of 2 m/s between commercially available hip protectors and inflatable devices. SIHP: Small inflatable hip protector under study, MIHP: Medium inflatable hip protector, LIHP: Large inflatable hip protector.

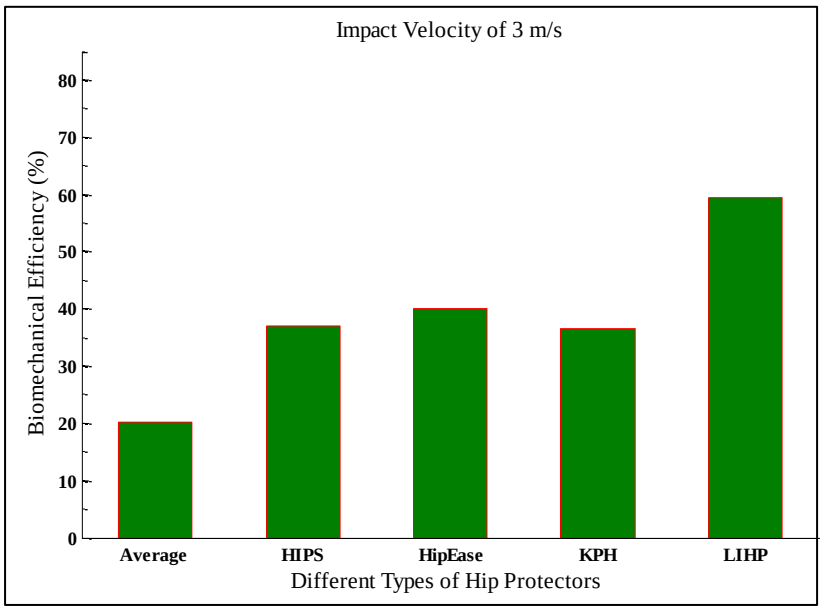

Figure 3- 6: Comparison of values for biomechanical effectiveness (attenuation in peak femoral force) at an impact velocity of 3 m/s between commercially available hip protectors and inflatable devices. Av: Average of biomechanical effectiveness of commercially available hip protectors at impact velocity of 3 ms, HIPS, HipEase , KPH®, are the most efficient types of commercially available hip protectors, LIHP: Large inflatable hip protector.

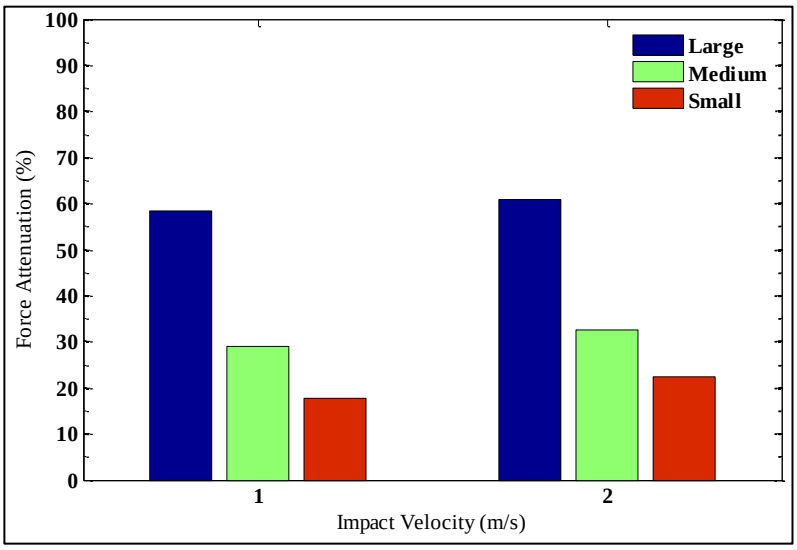

Figure 3- 7: Effect of surface area and impact velocity on force attenuation.

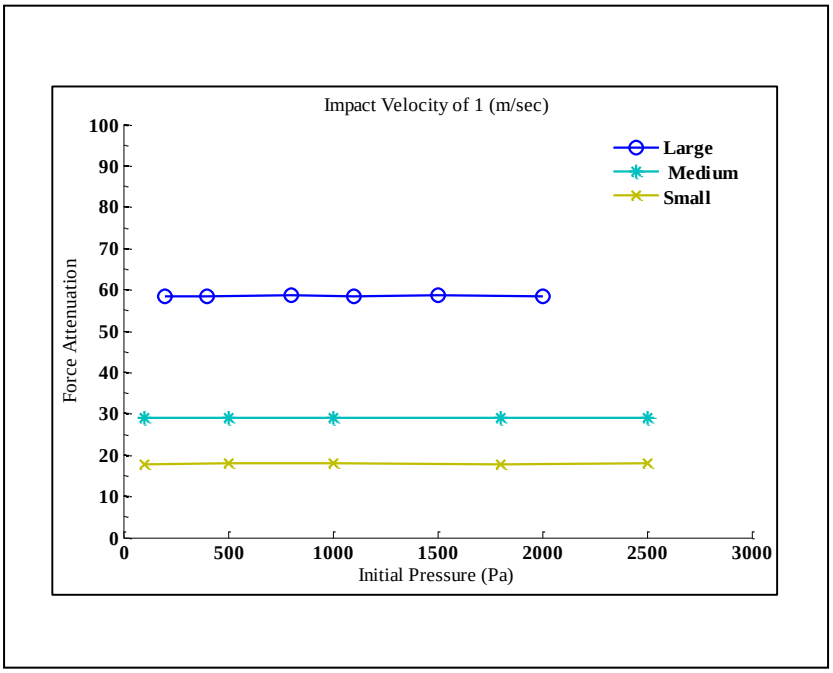

Figure 3- 8: Effect of initial pressure on biomechanical efficiency (force attenuation)

4: Deriving Mechanical Properties of Inflatable Hip Protectors of Different Sizes

In this chapter, first, fabrication of inflatable hip protectors is explained. Then the logarithmic decrement method is introduced as an effective way to extract mechanical properties – that is, stiffness and damping – of the systems. The procedure for running the tests is discussed next, and finally, the experimental results are compared with those of the extracted model outlined in Chapter 2.

4.1 Fabrication of inflatable hip protectors

I faced two main challenges in fabricating the inflatable hip protectors prototypes. First, the prototypes had to possess acceptable and reliable strength to impact forces in pelvis release experiments, as a bag explosion during impact test leads to damage to the experimental setup. Sturdy bags lower the risk of experimental damage and, more importantly, deliver more reliable data for consequent analysis. The second challenge was how to maintain a seal on the inflated hip protectors, given that uncontrolled leakage hinders data analysis and leads to inaccuracy in results.

To fabricate prototypes of inflatable hip protectors, different types of plastic bag of various thicknesses, and travel inflatable pillows of different materials, were used. The strength of the fabricated bags was examined, but it was concluded that plastic could not provide the desired tolerance against impact forces; it was not the proper material for this application, and bags made from it exploded at very low impact velocities – less than 1

m/sec. The same was observed for low-thickness travel pillows. Finally, I used a type of U-pattern travel pillow constructed of flocked vinyl. Experiments in pelvis release indicated that these are sturdy enough to tolerate impact forces at our desired impact velocities. The material provided much more strength than other initially tested materials such as plastic bags and some types of travel pillow that exploded in the early stages of experimental tests. I cut this U shape travel pillow into the size of my prototypes .

Sealing of the bag was the most challenging task when fabricating the prototypes, because the seal had to be strong and reliable to confine the air in our high impact velocity tests. To test the quality of sealing, the pressure inside the bag after each pelvis release experiment was examined. I took different approaches to seal the bags, including use of different types of glue, including crazy glue and epoxy, but none of these resulted in acceptable sealing. I also used hot glue gun plastic, which injects melted plastics to enclose and seal the bags. Although these showed good sealing, they could not maintain their pressure during a few trials. Then I fabricated two small plates with numerous small holes for bolt and screws, to enclose the bags but the sealing system under dynamic tests was not successful. Finally, I tried to seal the bag by heating and melting the bag membrane. In this approach, I used two irons and sealed the bags by heating two sides of the membrane simultaneously until they attached to each other. This method showed highly acceptable sealing as well as durability, so it was adopted for fabricating all prototypes.

Figure 4- 1: U-shape travel pillow used to fabricate inflatable hip protectors prototypes

4.2 Logarithmic decrement method

The force versus time curve resulting from each trial was used to determine the stiffness and damping of the inflatable hip protector using the logarithmic decrement method. First, I calculated the logarithmic decrement, δ, defined by [50]:

$$\delta = \ln\left(\frac{x(t)}{x(t+T)}\right) \tag{4- 1}$$

where x is displacement amplitude at time t, and T is the period of oscillation. The damping ratio was then given by

$$\zeta = \frac{\delta}{\sqrt{4\pi^2 + \delta^2}} \tag{4- 2}$$

The stiffness K was then determined from

$$\omega_d = \omega_n\sqrt{1 - \zeta^2} \tag{4- 3}$$

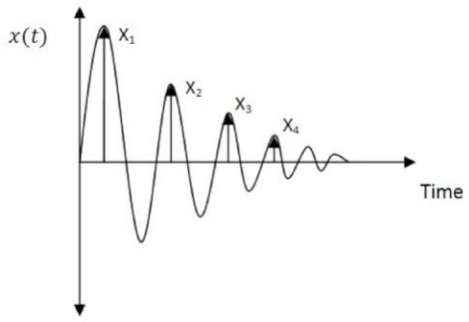

Figure 4- 2: Parameter definition used in logarithmic decrement method to determine mechanical properties of the system [50].

where $\omega_n = \sqrt{K/M}$ is the natural frequency and ω_d is the damped natural frequency. Consequently, damping constant *B* can be determined from

$$B = 2\zeta\sqrt{KM} \tag{4- 4}$$

4.3 Experimental procedure

The goal of these experiments was to measure the mechanical behaviour of the inflatable hip protector isolated from the underlying soft tissues. This study is important to assess the proposed mathematical model derived in Chapter 2. Accordingly, the surrogate pelvis (described in Chapter 3) was removed, and the impact pendulum, with effective mass 26 kg, was placed directly on top of the inflatable hip protector. Each inflatable hip protector was filled with air to an internal pressure of 250 Pa (gauge). A small excitation weight, mass 725 g, was then placed on top of the pendulum, and following a delay which allowed the system to become stable, the excitation weight was quickly removed, exciting the system into oscillation and facilitating identification of the effective stiffness and damping of the inflatable hip protector. Because the range of initial

pressure of the systems in the shaker setup and inverted pendulum are in different orders, it is not expected that the model proposed in Chapter 2 would predict accurately the results of the logarithmic decrement method. However, the experimental results are beneficial for assessing the proposed model.

4.4 Results

In Figure 4- 3, A, B and C display typical traces of force versus time for the large, medium, and small inflatable hip protectors, respectively.

Based on the measured natural frequency and logarithmic decrement, I calculated the stiffness and damping of each hip protector (Table 4-1). Stiffness increased with inflatable hip protector surface area, and damping was minimal – supporting my assumption of no damping in accordance with my mathematical models in Chapter 2.

Table 4- 3: Mean values of mechanical properties of inflatable hip protectors.

	Inflatable hip protector type		
	Large	Medium	Small
Stiffness (k-N/m)	56.23 (SD 0.8)	61.83 (SD 2.8)	72.77 (SD 1.9)
Damping Ratio	0.0223 (SD0.0041)	0.0234 (SD 0.0051)	0.029 (SD 0.0024)
Damping Constant (N-s/m)	53.28 (SD 9.5)	58.05 (SD 11.52)	78.8 (SD 5.7)
Undamped Natural Frequency (rad/s)	46.90 (SD 0.40)	49.60 (SD 0.81)	53. 88 (SD 0.71)
Damped Natural Frequency ((rad/s))	46.89 (SD 0.40)	49.58 (SD 0.80)	53. 86 (SD 0.71)

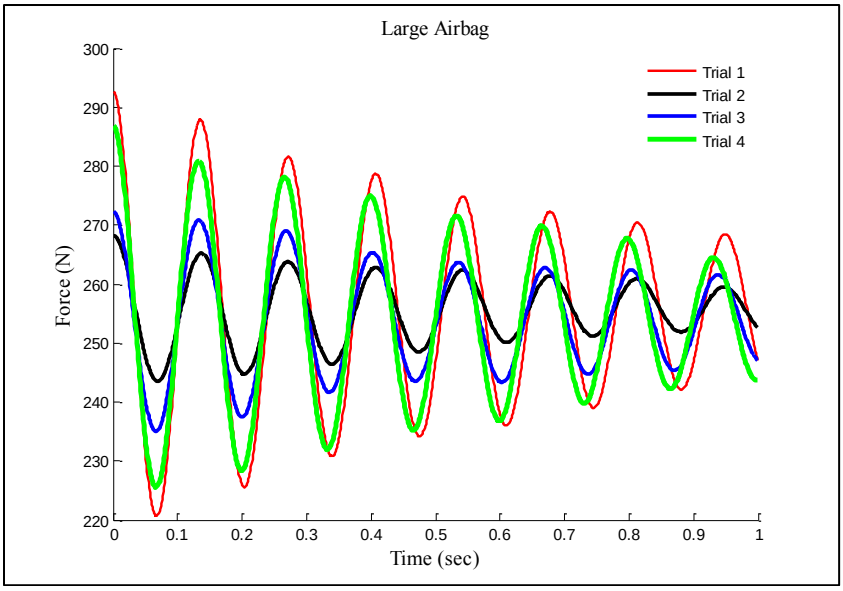
Large Airbag
Trial 1
Trial 2
Trial 3
Trial 4
Force (N)
Time (sec)
300
290
280
270
260
250
240
230
220
0
0.1
0.2
0.3
0.4
0.5
0.6
0.7
0.8
0.9
1

(A)

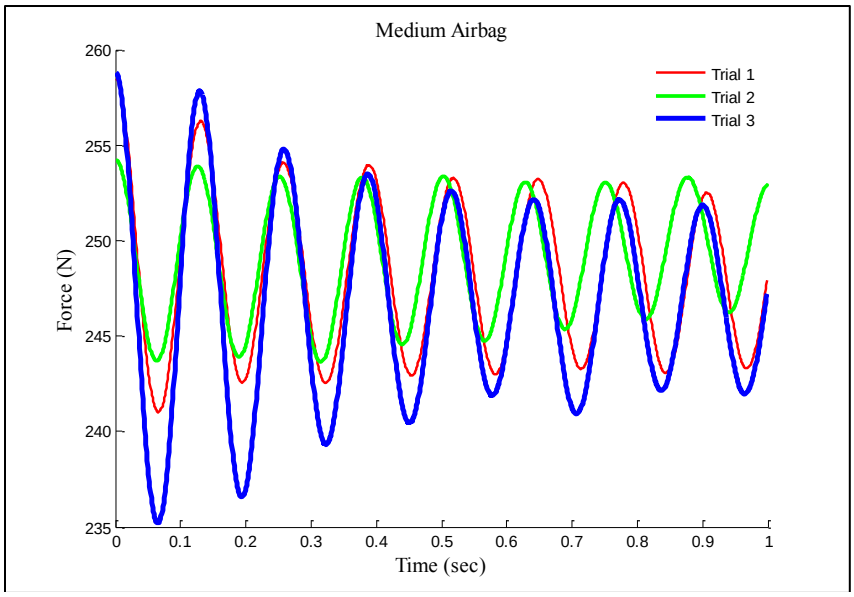
Medium Airbag
Trial 1
Trial 2
Trial 3
Force (N)
Time (sec)
260
255
250
245
240
235
0
0.1
0.2
0.3
0.4
0.5
0.6
0.7
0.8
0.9
1

(B)

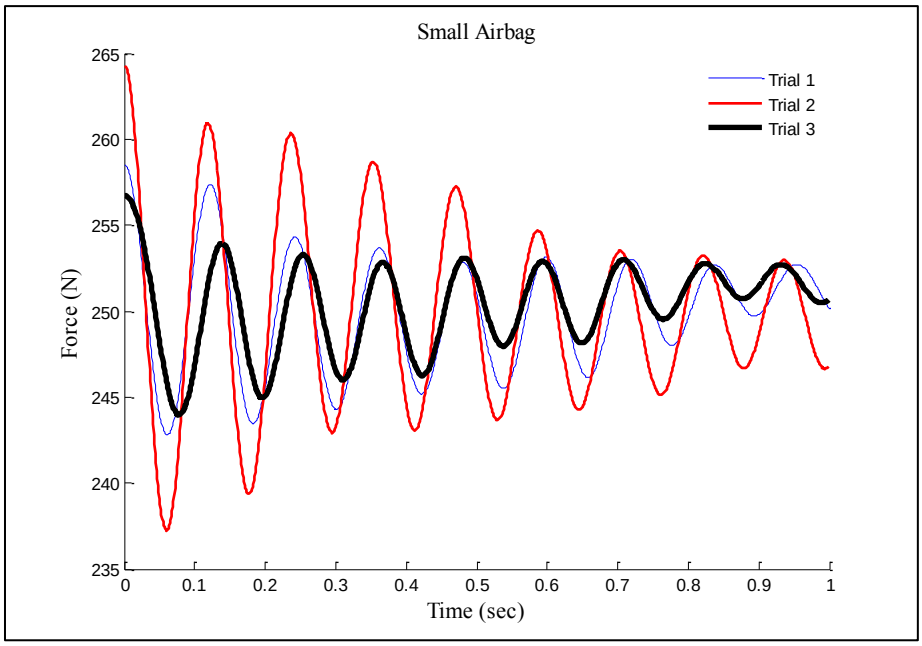

(C)

Figure 4- 3: Traces of force versus time for (A) large inflatable hip protector, (B) medium inflatable hip protector, and (C) small inflatable hip protector from experiments in which a small excitation mass was removed at t = 0. The traces were analysed to determine the effective stiffness and damping of each inflatable hip protector.

To validate the mathematical model derived in Chapter 2, the experimental and simulation effective area (A_e) of each inflatable hip protector are compared. Assuming $A_e = A_V$, from Equation (2- 23), one can write

$$K = \frac{nA_e{}^2(P_0 + \frac{M_e g}{A_e})}{A_e \Delta} \qquad (4\text{- }5)$$

where P_0 is the initial inflation pressure, M_e is the effective mass of the pendulum without the surrogate pelvis, and Δ is the thickness of the airbag measured by a clipper during experiments. Therefore, one can write

$$A_e = \frac{K\Delta - nM_e g}{P_0 n} \tag{4- 6}$$

where Δ is equal to 25, 20 and 15 mm for the large, medium, and small airbags respectively. Based on Equation 3-5, the effective areas are calculated as 74.2, 62.2, and 52 cm^2 which are consistent with the size of the bags shown in Figure 3- 4. The results suggest that even though the range of pressure in inverted pendulum experiments are considerably different than vibration tests in chapter 2, the model is still capable of providing approximate model behavior prediction in such higher initial pressure.

5: Conclusion and Future Work

The work described in this thesis can be considered a “first step” towards the design and manufacture of inflatable hip protectors, and this, the final chapter, describes the progress made towards achieving that goal. It also suggests the direction of future research along the path to developing and implementing suitable inflatable hip protectors for older people, to prevent or reduce the frequency of fall-related hip injuries.

In this first chapter, through authentic resources, I tried to indicate that the fall-related injuries are one of the most common causes of fatality among the elderly, and intervention to prevent such injuries is critical. I also introduced hip protectors as a promising intervention to reduce the risk of hip fracture. Finally, I introduced the understudy inflatable hip protectors, which are expected to provide great force attenuation along with considerable adherence among the elderly.

The second chapter was allocated to the study and observation of the mechanical behaviour of these types of hip protectors. Toward this end, a basic mathematical model of the system was developed, and for parameter identification and general model confirmation a series of dynamic tests as conducted. This study suggests that for small displacement variation, the system can be considered linear, with the stiffness depending strongly on initial pressure inside the bag.

In the third chapter, the biomechanical effectiveness of inflatable hip protectors was investigated. This study shows that airbags of moderate size provide over three times the force attenuation of current passive devices. These results support ongoing efforts to

develop inflatable hip protectors for older adults who are at high risk for falls and hip fracture.

In chapter four, fabrication of inflatable hip protector prototypes as one of the novelties in this study was described. And through different experimental configurations, a mechanical model of the system was investigated. Although, the tests were conducted at significantly higher initial pressure, the results indicated consistency with real situations.

In future work, however, some of the obstacles encountered in this study will be overcome. For example, fabrication of small and medium prototypes that can be tested by a pelvis-release experiments by introducing a low range of bag-burst risk effect of vent on biomechanical effectiveness. As the mathematical model suggests, it is expected that vented inflatable hip protectors will provide higher force attenuation during a fall. Future studies should also investigate a more complex range of surface geometries for product optimization, while the inflation method of airbags could be the next step in the research. This area of investigation is linked to the topic of ongoing research by several groups, which is the development of wearable sensor systems that can detect falls from daily activities such as sitting. It is important that, after inflatable hip protectors for the elderly have finally been implemented, acceptability of the devices by users be examined to assess their overall effectiveness.

6: References

1. Tinetti M (2003) Preventing falls in elderly persons. N Engl J Med 348: 42–49.

2. Tinetti M. E, Speechley M and Ginter S (1988) Risk factors for falls among elderly persons living in the community. N Engl J Med 319:1701-1707

3. Tinetti M and Speechley M (1989) Prevention of falls among the Elderly. N Engl J Med 320:1055-1059

4. Scott, V, Wagar, L, Elliott S (2010) Falls, Related Injuries among Older Canadians: Fall-related. Hospitalizations , Intervention Initiatives. Prepared on behalf of the Public Health Agency of Canada, Division of Aging and Seniors. Victoria BC: Victoria Scott Consulting.

5. SmartRisk (2010) Personal communication based on an extension of the study that provided data to The Economic Burden of Injury in Canada.

6. Empana JP, Dargent-Molina P and Breart G (2004) Effect of hip fracture on mortality in elderly women: the EPIDOS prospective study. Journal of the American Geriatrics Society, 52:685–690.

7. Wolinsky FD, Fitzgerald FT, and Stump TE (1997) The effect of hip fracture on mortality, hospitalization, and functional status: a prospective study. American Journal of Public Health and the Nation's Health. 87:398-403.

8. Norton R, Butler M, Robinson E, Lee-Joe T, Campbell AJ (2000). Declines in physical functioning attributable to hip fracture among older people: A follow-up study of case-control participants. Disability and Rehabilitation, 22: 345-351.

9. Hindmarsh JJ, Harvey E (1989) Falls in older persons causes and interventions. Arch Intern Med. 149:2217-2222.

10. Jaglal S, Sherry P, Schatzker J (1996). The impact and consequences of hip fracture in Ontario. Canadian Journal of Surgery 39, 105-111.

11. Papadimitropoulos E, Coyte P, Josse RGC (1997) Current and projected rates of hip fracture in Canada. Canadian Medical Association Journal 157, 1357-1363.

12. Van Staa AL, Visser A, Van der Zouwe N (2000) Caring for caregivers: experiences and evaluation of interventions for a palliative care team. Patient Education and Counselling 41, 93–105.

13. Misra D, Berry SD,. Broe KE, McLean RR, Cupples LA, Tucker KL, Kiel DP and Hannan MT (2011) Does dietary protein reduce hip fracture risk in elders? The Framingham osteoporosis study. Osteoporos Int 22:345–349

14. Lorincz, C, Manske S, and Zernicke RF (2009) Bone health: Part (1) Nutrition. Sports Health: A Multidisciplinary Approach 1: 253-260

15. Reginster JY, Seeman E, De Vernejoul MC (2005) Strontium ranelate reduces the risk of nonvertebral fractures in postmenopausal women with osteoporosis: treatment of peripheral osteoporosis (TROPOS) study. Journal of Clin Endocrinol Metab. 90:2816–22.

16. Laing AC, Tootoonchi I, Hulme PA, Robinovitch SN (2006) Effect of compliant flooring on impact force during falls on the hip. Journal of Orthopaedic Research 24 (7):1405–1411.

17. Kannus P, Parkkari, J, Niemi S, Pasanen, M, Palvanen M, arvinen M, Vuori I (2000) Prevention of hip fracture in elderly people with use of a hip protector. N. Engl. J. Med. 21, 1506–1513.

18. Brown A, Coyle D, Cimon K, Farrah K. (2008) Hip protectors in long-term care: a clinical and cost-effectiveness review and primary economic evaluation. Canadian Agency for Drugs and Technologies in Health

19. Singh S, Sun H, Anis AH (2004) Cost-effectiveness of hip protectors in the prevention of osteoporosis related hip fractures in elderly nursing home residents. Journal of Rheumatology 31 (8), 1607–1613.

20. Patel S, Ogunremi L, Chinappen U (2003) Acceptability and compliance with hip protectors in community-dwelling women at high risk of hip fracture. Rheumatology. 42:769-772.

21. Charpentier PJ (1996) A hip protector based on airbag technology. Bone 18:S117

22. Tamura T, Yoshimura T, Sekine M, Uchida M and Tanaka O (2009) A Wearable Airbag to Prevent Fall Injuries. IEEE Transaction on Information Technology in Biomedicine 13:913-914

23. Laing AC, Feldman F, Jalili M, Tsai MC, Robinovitch SN (2011) The effects of pad geometry and material properties on the biomechanical effectiveness of 26 commercially available hip protectors. Journal of Biomechanics, Journal of Biomechanics 44:2627-2635.

24. Hayes WC, Myers ER, Maitland LA, Resnick NM, Lipsitz, LA, Greenspan SL (1991) Relative risk for fall severity, body habits and bone density in hip fracture among the elderly. Trans. Orthop. Res. Soc. 16, 139.

25. Garrison JG, Slaboch CL, Niebur GL (2009) Density and architecture have greater effects on the toughness of trabecular bone than damage. Bone 44 /924–929

26. Courtney AC, Hayes WC, Gibson LJ (1996) Age-related differences in post-yield damage in human cortical bone: Experiment and model. Journal of Biomechanics 29:1463-1471

27. Weiner S and Wagner HD, The material bone: structure-mechanical function relations. Annu. Rev. Material Sci. 28:271–298.

28. Kopperdahl DL, Keaveny TM (1998) Yield strain behavior of trabecular bone. Journal of Biomechanics. 31:601-608

29. Lotz JC, Gerhart TN, Hayes WC, (1990). Mechanical properties of trabecular bone from the proximal femur: a quantitative CT study. Journal of Computer Assisted Tomography 14, 107–114.

30. Courtney AC, Wachtel EF, Myers ER, Hayes WC (1994) Effects of loading rate on strength of the proximal femur. Calcif Tissue Int 55: 53–58.

31. Robinovitch SN, Evans SL, Minns J, Laing AC, Kannus P, Cripton PA, Derler S, Birge SJ, Plant D and Cameron ID (2009) Hip protectors: recommendations for biomechanical testing (part I). Osteoporosis Internatioonal, 20:1977-1988

32. Lotz J C, Hayes WC (1990). The use of quantitative computed tomography to estimate risk of fracture of the hip from falls. The Journal of Bone and Joint Surgery 72:689-700

33. Courtney AC, Wachtel EF, Myers ER, Hayes WC (1995). Age-related reductions in the strength of the femur tested in a fall-loading configuration. The Journal of Bone and Joint Surgery. American 77:387-95

34. Pinilla, TP, Boardman KC, Bouxsein ML, Myers ER, Hayes WC (1996) Impact direction from a fall influences the failure load of the proximal femur as much as age-related bone loss. Calcified Tissue International 58, 231-235.

35. Pulkkinen P, Eckstein F, Lochmuller EM, Kuhn V, Jamsa T (2006) Association of geometric factors and failure load level with the distribution of cervical vs. trochanteric hip fractures. J Bone Miner Res 21:895–901

36. Cole HJ and Van der Meulen MCH (2010) Osteoporosis: Biomechanics of Bone (Chapter 7).

37. Nankaku M, Kanzaki H, Tsuboyama T and Nakamura T (2005) Evaluation of hip fracture risk in relation to fall direction. Osteoporosis International 16:1315-1320.

38. Robinovitch SN, Hayes WC, McMahon TA (1997) Predicting the Impact Response of a Nonlinear Single-Degree-of-Freedom Shock-Absorbing System From the Measured Step Response; Journal of Biomechanical Engineering 119:221-228

39. Cha PD, Rosenberg JJ, and Dym CL (2000) Fundamentals of Modeling and Analyzing Engineering Systems, Cambridge University Press, New York.

40. Chaikin D (1991) How It Works-Airbags, Popular Mechanics : 81-82.

41. Grajnert J and Krettek O (1991) Zur Phanomenologie und Estrastzmodellbildung von Lufifedern, ZEV+DET Glas, Ann. 115, Nr. 7/8

42. Shimozawa K and Tohtake T (2008) An air spring model with non-linear damping for vertical motion, Quarterly Report of RTRI 49: 209-214

43. Clyde LL (1936) Thermodynamics: the principles of thermodynamics and their application to engineering processes:1891-1972

44. Williams RA (1997). Automotive active suspensions part 2: practical considerations. Proc. IMechE, Part D: J. Automobile Engineering, 211, 427−444.

45. Feldman F, Robinovitch SN (2007) Reducing hip fracture risk during sideways falls: evidence in young adults of the protective effects of impact to the hands and stepping. J Biomech 40:2612–2618

46. Berg M (1999) A Three-Dimensional Air-spring Model with Friction and Orifice Damping," Proceedings of the 16th IAVSD Symposium on the Dynamics of Vehicles on Roads and Tracks, Pretoria, South Africa. Journal of Vehicle System Dynamics, 33.

47. Oda N and Nishimura S (1970) Vibration of Air Suspension Bogies and Their Design," Bulletin of JSME,13:55-58.

48. Robinovitch SN, Hayes WC, McMahon TA (1997) Distribution of contact force during impact to the hip. Ann Biomed Eng, 25:499–508.

49. Ogata K (2002) Modern Control Engineering. Prentice-Hall, Inc., fourth edition : 497-450

50. Inman DJ, Engineering Vibrations (2001) 2nd ed. Upper Saddle River, NJ: Prentice-Hall.

51. Laing AC, Feldman F, Jalili M, Tsai CM, Robinovitch SN (2011) The effects of pad geometry and material properties on the biomechanical effectiveness of 26 commercially available hip protectors. Journal of Biomechanics. doi:10.1016/

52. Laing AC, Robinovitch SN (2008) Effect of soft shell hip protectors on pressure distribution to the hip during sideways falls. Osteoporosis International 19:1067–1075.

53. Laing AC, Robinovitch SN (2008) The force attenuation provided by hip protectors depends on impact velocity, pelvic size, and soft tissue stiffness. Journal of Biomechanical Engineering 130: 061005–061009.

54. Mills NJ, (1996) The biomechanics of hip protectors. Proceedings of the Institution of Mechanical Engineers. Part H, Journal of Engineering in Medicine 210: 259–266.

55. Robinovitch SN, Hayes WC, McMahon TA, (1997) Distribution of contact force during impact to the hip. Annals of Biomedical Engineering 25, 499–508.

56. Laing AC, Robinovitch SN (2010) Characterizing the effective stiffness of the pelvis during sideways falls on the hip. Journal of Biomechanics 43, 1898–1904.